

Rotational and vibrational excitations in ^{84}Zr studied through in-beam and ^{84}Nb β -decay spectroscopy

J. Döring,^{1,2,3} R. A. Kaye,^{3,*} A. Aprahamian,² M. W. Cooper,^{3,†} J. Daly,² C. N. Davids,⁴ R. C. de Haan,² J. Görres,² S. R. Leshner,² J. J. Ressler,^{5,‡} D. Seweryniak,^{4,5} E. J. Stech,² A. Susalla,² S. L. Tabor,³ J. Uusitalo,^{4,§} W. B. Walters,⁵ and M. Wiescher²

¹*Gesellschaft für Schwerionenforschung mbH, 64291 Darmstadt, Germany*

²*Department of Physics, University of Notre Dame, Notre Dame, Indiana 46556*

³*Department of Physics, Florida State University, Tallahassee, Florida 32306*

⁴*Physics Division, Argonne National Laboratory, Argonne, Illinois 60439*

⁵*Department of Chemistry, University of Maryland, College Park, Maryland 20742*

(Received 5 July 2002; published 23 January 2003)

Low- and medium-spin states have been investigated in the even-even nucleus ^{84}Zr by using in-beam γ -ray spectroscopy via the reactions $^{59}\text{Co}(^{28}\text{Si},p2n)$ and $^{58}\text{Ni}(^{32}\text{S},\alpha2p)$ at beam energies of 99 and 135 MeV, respectively. Several new levels have been identified, including a new even-spin sequence of the γ -vibrational band. The previously known sequence has been found to be built on a 3^+ state at 1575.3 keV representing the odd-spin sequence. In addition, the β^+ /EC decay of mass-separated ^{84}Nb sources has been studied by β - and γ -ray spectroscopy following the bombardment of a thin ^{58}Ni target with ^{28}Si ions at 94 MeV. Some low-lying daughter states up to spin and parity of 4^+ have been identified in ^{84}Zr , and a half-life of 9.5 ± 1.0 s has been measured for the ^{84}Nb ground-state decay. The systematics of γ -vibrational states in even-even Zr nuclei and a comparison with model predictions indicate increasing γ softness and triaxiality as the spherical neutron shell closure at $N=50$ is approached. Using an empirical estimate, a triaxiality of about 25° has been extracted for ^{84}Zr . Furthermore, a negative-parity structure of 4^- and 6^- states which is similar to other $N=44$ isotones has been identified in ^{84}Zr as a two-quasineutron excitation.

DOI: 10.1103/PhysRevC.67.014315

PACS number(s): 21.10.Re, 23.20.En, 23.20.Lv, 27.50.+e

I. INTRODUCTION

High-spin states of some neutron-deficient even-even Zr isotopes have been studied extensively in the past, and interesting features have been identified in ^{84}Zr , such as a substantial quadrupole deformation of $\beta_2 \approx 0.4$ interpreted as rigid rotation [1], $g_{9/2}$ quasiproton and $g_{9/2}$ quasineutron alignments [2,3] along the yrast line, competition of vibrational and rotational collectivity [4], superdeformation at very high spins [5,6], and band termination [7].

In recent years there has been increasing interest in examining the relationship between collective rotations and vibrational excitations for the neutron-deficient nuclei in the mass-80 region. Neutron number 44 has been found to be at the borderline where rotational and vibrational collectivities interchange their dominance in the excitation spectrum; i.e., the even-even nucleus $^{84}\text{Zr}_{44}$ has been considered to show evidence for rigid rotation [1] which has recently been verified, e.g., by another measurement of magnetic dipole moments of low-lying states [8], while the yrast states in $^{86}\text{Zr}_{46}$

depopulate by weakly enhanced $E2$ transitions with $B(E2)$ strengths of about 7 Weisskopf units (W.u.) for the low-spin states [9] and about 14 W.u. for the high-spin states [10], indicating the presence of vibrational excitations.

A large quadrupole deformation was deduced for ^{84}Zr from an early level lifetime measurement [1]. Subsequent lifetime measurements of the lowest yrast states, however, provided a wide time range in particular for the 2^+ yrast level, from 14.4(7) ps [11] to 24(2) ps [3]. The latest results [3] indicate a smaller quadrupole deformation along the positive-parity yrast band, yielding an average value of $B(E2)=32$ W.u. for the $E2$ transition strengths between states up to the 8^+ level and, thus, a weakening of the rigid rotor picture. Further, the energy ratios of $E(4^+)/E(2^+) = 2.34$ and $E(6^+)/E(2^+) = 3.96$ as deduced from the low-lying yrast levels in ^{84}Zr deviate substantially from the rigid rotor limit of 3.33 and 7.0, respectively. Hence, vibrational collectivity may still affect the low-spin states. Early potential-energy surface calculations [6] suggested an almost spherical shape for ^{84}Zr in its ground state, with the evolution of a deformed triaxial shape at low angular momenta. Thus, to explore the evolution of the nuclear shape as a function of excitation energy and angular momentum in a more complete way, the present study of low-lying and/or nonyrast states in ^{84}Zr has been initiated.

Furthermore, an inspection of the published ^{84}Zr level schemes revealed that the weakly populated high-spin band built on the second 2^+ state at 1119 keV (γ -vibrational band) becomes yrast at the 14^+ 6250 keV level [4,5], which is in sharp contrast to the strong population of the 14^+ state

*Present address: Department of Chemistry and Physics, Purdue University Calumet, Hammond, IN 46323.

†Present address: National Superconducting Cyclotron Laboratory, Michigan State University, East Lansing, MI 48824.

‡Present address: Wright Nuclear Structure Laboratory, Yale University, New Haven, CT 06520.

§Present address: Accelerator Laboratory, University of Jyväskylä, FIN-40351 Jyväskylä, Finland.

at 6304 keV. The latter state has been assigned as a member of the yrast-state band. This suggests a spin assignment problem along the level sequence built on the second 2^+ state and could be related to the missing 3^+ state which is present in most of the even-even nuclei in the mass-80 region but not yet observed in ^{84}Zr . Thus, a reinvestigation of the low- to medium-spin structure of ^{84}Zr may also contribute to resolve this discrepancy.

Two different kinds of experiments have been initiated to gather nuclear structure information on ^{84}Zr . First, an in-beam study of ^{84}Zr has been performed with a five-Ge-detector array at Florida State University, and second, a mass-separated $^{84}\text{Nb} \rightarrow ^{84}\text{Zr}$ decay study has been carried out by using fast “in-flight” separation provided by the Argonne fragment mass analyzer (FMA) [12]. Here a setup of three Ge detectors combined with three plastic scintillators was used to record γ and β radiations.

Previously, the ground state of the nucleus ^{84}Nb was found to decay with a half-life of 12 ± 3 s and states up to the 4^+ yrast level in ^{84}Zr were identified [13]. Thus, a (3^+) assignment was suggested [14] for the ^{84}Nb ground state. This moderate spin and the relatively large Q_{EC} value of 9610 keV deduced from systematics [15] promised the β -delayed population of many nonyrast states in ^{84}Zr .

II. EXPERIMENTAL TECHNIQUES

A. In-beam coincidence measurements

The low- to medium-spin structure of ^{84}Zr was studied via in-beam experiments through two different reactions, the $^{59}\text{Co}(^{28}\text{Si}, p2n)$ and the $^{58}\text{Ni}(^{32}\text{S}, \alpha 2p)$ reactions, at beam energies of 99 and 135 MeV, respectively. The ion beams were provided by the Florida State University Tandem-Superconducting Linac facility.

In the first experiment a metallic ^{59}Co foil (100% natural abundance) with a thickness of 10.6 mg/cm^2 was used as target. In the second experiment, the target was a ^{58}Ni foil isotopically enriched to over 99% and about 20 mg/cm^2 thick. In both experiments, the emitted γ rays were recorded with a setup of five Compton-suppressed Ge detectors, each about 25% relative efficiency, combined with a low-energy photon spectrometer (LEPS). Three Ge detectors and the LEPS were placed at 90° relative to the beam direction and two Ge detectors at a backward position of 145° .

Twofold or higher coincidence data were stored in list mode on 8 mm tape and subsequently analyzed using standard in-house software [16]. From each measurement, triangular and square matrices were generated with different energy dispersions. The triangular matrices contained all Ge-detector coincidence events and were used to construct the level scheme of ^{84}Zr , while the square matrices, where the events from the backward detectors were sorted against the 90° events, were analyzed with respect to directional correlations of oriented nuclei (DCO) to help in spin assignments. The DCO ratio was determined from the experimental intensities of a selected γ transition as deduced from coincidence spectra gated by a low-lying $\Delta I=2$ transition at 145° and 90° according to the relation $R_{\text{DCO}} = I_\gamma(145^\circ)/I_\gamma(90^\circ)$.

In general, the DCO ratio depends on the initial and final spins and on the mixing ratio of different multipoles in the gating and the transition of interest, as well as on the degree of nuclear alignment. When a gate is set on a stretched $E2$ transition, then the interpretation of the experimental ratio is most straightforward. In this case, a DCO ratio of about 0.5 is expected for a pure $\Delta I=1$ dipole transition and 1.0 for a stretched $\Delta I=2$ transition based on the geometry of the FSU Ge-detector array. For a mixed $\Delta I=1$ transition, the ratio may vary between 0.2 and 1.8 as a function of the dipole-quadrupole mixing and the amount of nuclear alignment. Ambiguities may also occur since an unstretched pure $\Delta I=0$ transition is expected to have a ratio slightly larger than unity; i.e., similar to a stretched $E2$ transition [17].

DCO ratios have been deduced whenever possible from the statistics in the gated coincidence spectra. However, for some strong transitions between high-spin states, the large Doppler-shifted peaks prevented a clear extraction of the line intensities. The γ -ray energies, relative intensities, and DCO ratios of transitions assigned to ^{84}Zr have been compiled in Table I.

B. Angular distribution measurement

An angular distribution measurement was performed via the $^{58}\text{Ni}(^{32}\text{S}, \alpha 2p)^{84}\text{Zr}$ reaction at 130 MeV beam energy. The Compton-suppressed Ge detector having an energy resolution of 1.9 keV at 1332.5 keV was placed about 15 cm away from the target. Singles spectra were measured at angles of 0° , 30° , 45° , 60° , and 90° relative to the beam direction. The yields were normalized by the live-time-gated, integrated beam current. The peak areas of the transitions of interest were deduced from each spectrum by means of a least-squares fitting procedure using (mostly) symmetric Gaussian curves for the description of the γ line shapes. The angular distribution function $W(\Theta) = A_0[1 + a_2P_2(\cos \Theta) + a_4P_4(\cos \Theta)]$ was fitted to the normalized peak intensities, where $P_k(\cos \Theta)$, $k=2, 4$, are the Legendre polynomials. The resulting angular distribution coefficients a_2 and a_4 for some transitions in ^{84}Zr are compiled in Table II. Only those γ lines are reported which are known from the coincidence measurement (performed via the same reaction) to form a single peak or part of a complex group which could be reliably decomposed. For the strongest transitions in ^{84}Zr , the deduced coefficients are in fair agreement with previously reported values [4,8]. In case of poor statistics and/or large a_4 uncertainty, the fit was restricted to the a_2 coefficient only.

C. Decay measurement

A number of nuclei were produced by bombarding a 1.0 mg/cm^2 ^{58}Ni target with a 94 MeV beam of ^{28}Si ions provided by the ATLAS facility at Argonne National Laboratory. The $A=84$ recoils were separated from other reaction products using the FMA [12] and implanted onto aluminized Mylar tape located just behind the focal plane position. After a deposition time of 20 s, the tape was moved to a counting station approximately 1 m away from the focal plane and

TABLE I. Energy, spin, and parity of initial and final states, and energy, relative intensities, and DCO ratios for γ transitions assigned to ^{84}Zr .

E_{lev} (keV)	I_i^π	I_f^π	E_γ ^a (keV)	I_γ ^b	R_{DCO} ^b	I_γ ^c	R_{DCO} ^c
Band 3							
539.8	2 ⁺	0 ⁺	539.8(1)	100(3) ^d	1.03(3)	100(3) ^d	1.04(4)
1262.7	4 ⁺	2 ⁺	722.9(1)	81(2)	1.01(3) ^e	79(2)	0.97(4) ^e
2136.3	6 ⁺	4 ⁺	873.6(1)	55(2)	1.03(4)	55(2)	0.99(5)
3088.8	8 ⁺	6 ⁺	952.5(1)	38(1)	0.98(5)	32(2)	0.95(7)
4068.5	10 ⁺	8 ⁺	979.7(2)	30(1)	1.04(6)	24(2)	1.03(7)
5135.8	12 ⁺	10 ⁺	1067.3(2)	24(1)	0.99(7)	16(1)	0.94(9)
6302.1	14 ⁺	12 ⁺	1166.3(3)	11(1)	0.93(12)	7.1(5)	
7497.9	16 ⁺	14 ⁺	1195.8(3)	8(1)		5.4(6)	
8744	18 ⁺	16 ⁺	1246(1)	3(1)		1.5(6)	
Band 2							
4587.4	(10 ₂ ⁺)	10 ⁺	518.9(3)	2.5(4)	0.74(12)	2.2(6)	
		8 ⁺	1499(1)	1.5(4)		≈ 1	
5615	(12 ₂ ⁺)	(10 ₂ ⁺)	1028(1)	≈ 1		≈ 1	
6643	(14 ₂ ⁺)	(12 ₂ ⁺)	1028(1)	≈ 1		≈ 1	
		(12 ⁺)	1507.6(3)	2.7(4)		2.8(3)	
7857	(16 ₂ ⁺)	(14 ₂ ⁺)	1213(1)	≈ 1		≈ 1	
		14 ⁺	1555(1)	1.5(4)		≈ 1	
Band 1, even							
1119.2	2 ₂ ⁺	2 ⁺	579.3(1)	5.6(6)	1.29(10)	8.9(6)	1.02(11)
		0 ⁺	1119.3(2)	2.6(4)		3.1(4)	
1887.6	4 ₂ ⁺	3 ⁺	312.2(3)	0.4(2)		≈ 1	
		4 ⁺	625.2(3)	0.5(3)		≈ 1	
		2 ₂ ⁺	768.5(3)	1.4(2)		3.1(4)	0.91(17)
2739.6	6 ₂ ⁺	6 ⁺	603(1)	0.2(1)		≈ 1	
		4 ₂ ⁺	852(1)	0.9(3)		≈ 1	
Band 1, odd							
1575.3	3 ⁺	2 ₂ ⁺	456.2(1)	3.2(3)	0.97(10)	8.2(5)	1.02(10)
		2 ⁺	1035.8(2)	2.1(4)	0.96(10)	4.9(5)	1.09(21)
2335.1	5 ⁺	3 ⁺	759.8(2)	3.4(3)	1.05(18)	6.1(4)	0.94(12)
		4 ⁺	1072.4(3)	1.1(3)	0.43(18)	1.9(3)	
3202.0	7 ⁺	5 ⁺	866.9(2)	3.9(4)	1.08(11)	5.0(5)	1.15(19)
4137.4	9 ⁺	7 ⁺	935.4(3)	2.8(3)	1.04(15)	3.2(5)	1.12(24)
5150.1	11 ⁺	9 ⁺	1012.7(5)	4(2)	0.95(16)	4(2)	
6248.2	13 ⁺	11 ⁺	1098.1(4)	1.7(3)	1.05(21)	2.2(3)	
7299.8	(15 ⁺)	(14 ₂ ⁺)	656.4(4)	3.2(4)	0.26(7)	2.8(4)	0.47(15)
		13 ⁺	1051.9(6)	1.4(4)		2.4(4)	
8499	(17 ⁺)	(15 ⁺)	1199(1)	≈ 1		≈ 1	
Band 4							
2825.8	5 ⁻	4 ⁺	1563.1(3)	15(1)	0.54(7)	15(1)	0.63(9)
3493.8	7 ⁻	6 ⁻	415.0(2)	1.1(3)	0.25(10)	1.1(2)	0.51(18)
		5 ⁻	667.9(2)	1.9(2)	1.22(24)	2.5(4)	
		6 ⁺	1357.5(3)	12(1)	0.56(7)	11(1)	0.54(8)
3551.7	7 ₂ ⁻	6 ⁻	473(1)	≈ 1		≈ 1	
		5 ⁻	726.4(4)	1.4(3)		1.5(3)	
		6 ⁺	1415.5(4)	4.6(6)	0.40(11)	4.1(5)	0.50(21)
3722	(7 ₃ ⁻)	6 ⁺	1586(1)	≈ 1		≈ 1	
4378.5	9 ⁻	(7 ₃ ⁻)	656(1)	≈ 1		≈ 1	
		7 ₂ ⁻	826.9(3)	2.0(4)	1.04(24)	1.3(5)	1.14(19)

TABLE I. (*Continued*).

E_{lev} (keV)	I_i^π	I_f^π	E_γ^a (keV)	I_γ^b	R_{DCO}^b	I_γ^c	R_{DCO}^c
		7^-	884.7(2)	9.4(5)	0.99(9)	7.6(5)	0.93(13)
		8^+	1289.6(4)	0.7(3)		1.1(3)	
5316.4	11^-	9^-	937.9(2)	11(1)	1.00(9)	7.0(5)	1.08(14)
6324.5	13^-	11^-	1008.1(3)	9.9(7)	1.01(9)	6.7(6)	0.94(14)
7410.9	15^-	13^-	1086.4(3)	5.1(6)	0.86(16)	4.0(4)	1.0(3)
8608	17^-	15^-	1197(1)	2(1)		≈ 1	
Band 5							
2810.8	4^-	5^+	475.3(5)	1.1(3)		≈ 1	
		4_2^+	922.9(4)	1.5(7)		2.0(4)	
		3^+	1235.6(2)	1.8(3)		2.6(3)	0.62(11)
		4^+	1548(1)	≈ 1		≈ 1	
3078.8	6^-	5^-	253.1(2)	1.4(2)		1.3(2)	0.58(14)
		4^-	267.7(2)	2.6(2)		2.8(3)	1.05(17)
3313.3	6_2^-	5^-	487.5(1)	7.8(4)	0.29(4)	7.8(5)	0.35(6)
4036.7	8^-	7^-	543.1(2)	3.0(3)	0.28(6)	2.7(4)	0.34(12)
		6_2^-	723.3(3)	≈ 8	1.01(3) ^e	≈ 6	0.97(4) ^e
		6^-	957.9(3)	1.3(4)		1.1(3)	
4869.2	10^-	9^-	490.6(3)	1.3(2)	≤ 0.2	1.0(3)	
		8^-	832.5(1)	12(1)	0.92(9)	8.3(5)	1.08(13)
5785.3	12^-	11^-	470(1)	1.3(4)		1.6(4)	
		10^-	916.1(2)	10(1)	0.94(11)	7.4(7)	0.92(17)
6797.4	14^-	12^-	1012.1(5)	5(2)	0.85(9)	4(1)	
7929.3	16^-	14^-	1131.9(5)	2.6(5)	0.88(15)	2.9(4)	
9196	18^-	16^-	1267(1)	3(1)		2(1)	

^aUncertainty is given in parentheses in units of the last digit.

^bReaction $^{58}\text{Ni}(^{32}\text{S}, \alpha 2p)^{84}\text{Zr}$. DCO ratios have been deduced from gates set on low-lying $E2$ transitions.

^cReaction $^{59}\text{Co}(^{28}\text{Si}, p 2n)^{84}\text{Zr}$.

^dNormalization.

^eDCO ratio is given for the doublet.

counted for a period of 20 s. The emitted γ rays were detected with three high-purity Pb-Cd-shielded Ge detectors (55% relative efficiency) surrounding the plastic pipe which housed the moving tape in close geometry. All three Ge detectors had a thin (≈ 3 mm) plastic scintillation detector in front to record positrons emitted during the decay. Gamma-ray spectra were recorded with the Ge detectors (which had thin Be windows) in the energy range 20–2000 keV. Singles and coincidence events were tagged by an electronic time signal and written in list mode on magnetic tape. Measurements were also made with deposition and counting times of 6 s to enhance the number of counts for shorter lifetimes. The measured events were sorted off-line into β - γ , β - γ - γ , γ - γ , time- γ , and β -gated time- γ matrices. Also, the events from the 6 s counting cycles were added to the events from the 20 s cycles to improve the statistics. Energy calibration was done using well-known background lines, in particular the lines from the $^{113}\text{Cd}(n, \gamma)^{114}\text{Cd}$ reaction which are known with high precision [18]. An efficiency calibration was performed with very weak radioactive sources of ^{152}Eu , ^{56}Co , ^{228}Th , and ^{182}Ta to minimize pileup and dead-time effects.

TABLE II. Results of the angular distribution measurement for γ rays assigned to ^{84}Zr . Listed are transition energy, spin and parity of initial and final states, angular distribution coefficients, and proposed multipolarity.

E_γ (keV)	I_i^π	I_f^π	a_2	a_4	Multipolarity
267.7	6^-	4^-	0.21(7)	0.04(7)	$E2$
456.2	3^+	2_2^+	0.23(12)	0.09(12)	$M1/E2$
487.5	6_2^-	5^-	-0.53(11)	-0.09(12)	$M1/E2$
539.8	2^+	0^+	0.23(1)	-0.03(1)	$E2$
543.1	8^-	7^-	-0.75(8)	0.06(9)	$M1/E2$
579.3	2_2^+	2^+	-0.12(6)	0.02(7)	$M1/E2$
722.9	4^+	2^+	0.29(2) ^a	-0.03(3) ^a	$E2$
759.8	5^+	3^+	0.36(8)	-0.09(8)	$E2$
768.5	4_2^+	2_2^+	0.13(8)		$E2$
866.9	7^+	5^+	0.35(10)	-0.22(10)	$E2$
873.6	6^+	4^+	0.32(2)	-0.07(2)	$E2$
937.9	11^-	9^-	0.28(6)	-0.03(6)	$E2$
979.7	10^+	8^+	0.20(5)	-0.05(6)	$E2$
1357.5	7^-	6^+	-0.30(9)		$E1$
1563.1	5^-	4^+	-0.43(7)	0.17(8)	$E1$

^aCoefficients are given for the 722.9-723.3 keV doublet.

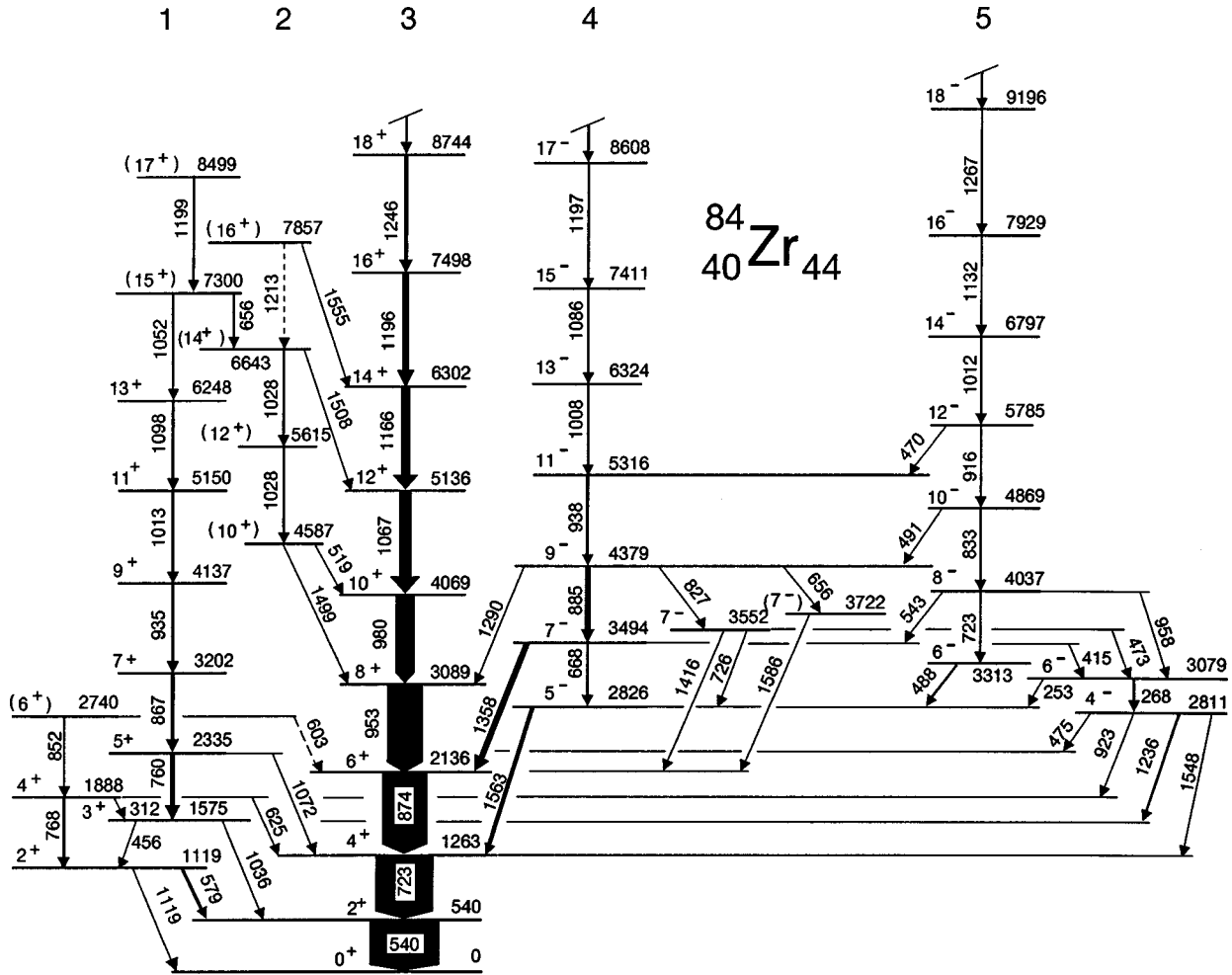


FIG. 1. Level scheme of ^{84}Zr as deduced from the present in-beam measurements. The bands labeled with 3, 4, and 5 have been observed to higher levels in previous work [5].

III. LEVEL SCHEME

A. States in ^{84}Zr deduced from in-beam measurements

The low- to medium-spin level scheme of ^{84}Zr as deduced from our in-beam measurements is shown in Fig. 1. Several new levels and transitions have been introduced based on our $\gamma\text{-}\gamma$ coincidence data. As an example, the γ -ray spectra in coincidence with two low-lying yrast transitions are shown in Fig. 2. In some cases previously reported spin assignments have been challenged. Our arguments for the changes will be discussed below.

1. γ -vibrational band

The γ -vibrational band is built on the second 2^+ state at 1119.2 keV. The previously reported [1,2,4] coincidence relationships have been confirmed; i.e., the 456.2 keV transition has been found to depopulate the level at 1575.3 keV. This transition is in strong coincidence with all transitions of the known feeding sequence, confirming the reported placement of this side structure.

The measured DCO ratios and the angular distribution coefficients of the 456.2 keV transition (see Fig. 3) could be interpreted as a $\Delta I=2$ transition leading to a possible spin-4

assignment to the level at 1575.3 keV, as previously suggested [1,4,5]. However, our measured results are also compatible with the assumption of a mixed dipole-quadrupole nature for the 456.2 keV transition. Our DCO ratios and angular distribution coefficients for the 456.2 keV transition are compatible with a $3^+ \rightarrow 2^+$ assignment. A dipole-quadrupole mixing of $\delta \approx 0.7$ can be determined for this transition which yields an $E2$ admixture of at least 33%. Systematics of the $3^+ \rightarrow 2_2^+$ transition of even-even nuclei in the mass-80 region show that a similar high $E2$ admixture occurs quite often, e.g., in ^{80}Kr (90% $E2$ [19]) or ^{78}Se (17% $E2$ [20]).

The measured DCO ratio for the depopulating 1035.8 keV transition is also not conclusive since pure $E2$ or mixed $\Delta I=1$ characters are possible. This situation is very similar to the one found in ^{82}Sr [21] where the extracted DCO ratios for the corresponding transitions are also close to unity. Only the DCO ratio for the 1235.6 keV $E1$ transition indicates a clear $\Delta I=1$ nature. Since the spin of the 2810.8 keV level has been established to be 4 through the DCO ratio of the feeding 267.7 keV transition (see Sec. III A 2), a spin of 3 is deduced for the 1575.3 keV level. For the intraband transitions at 759.8, 866.9, and 935.4 keV, DCO ratios of close to

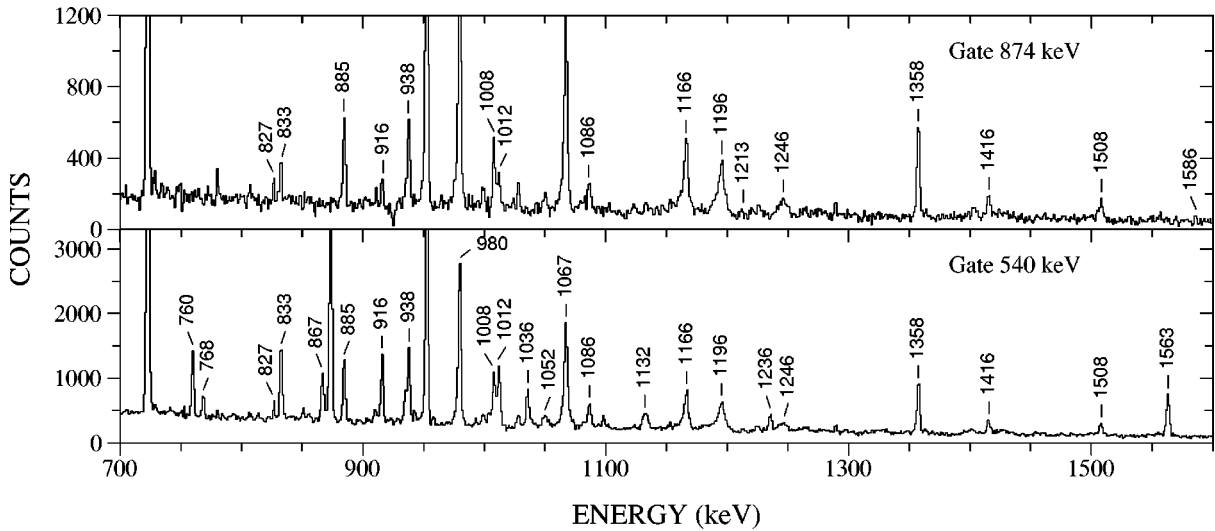


FIG. 2. Background-corrected γ -ray spectra in prompt coincidence with the 540 and 874 keV transitions of the yrast sequence in ^{84}Zr .

unity have been extracted, supporting the $E2$ assignments reported earlier. Thus, the DCO ratios lead to an odd-spin assignment to the known decay sequence.

Further, new transitions at 768.5 and 852 keV have been found to feed into the second 2^+ state at 1119.2 keV. The new 768.5 keV line can be seen in the higher-energy portion

of the 540 keV gate displayed in Fig. 2. Thus, a new level at 1887.6 keV has been identified which is weakly populated by an 852 keV transition, leading to a new level at 2740 keV. This level also decays by a weak 603 keV line to the yrast 6^+ state. The DCO ratio and angular distribution for the 768.5 keV line indicate $\Delta I=0$ or 2. The weak connection to

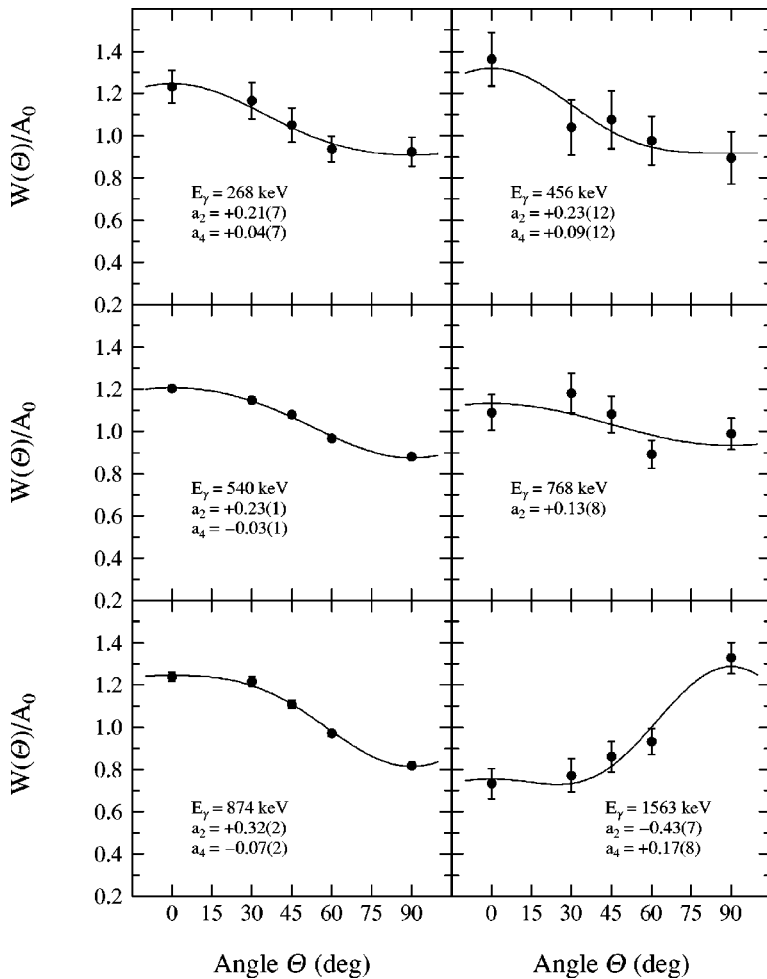


FIG. 3. Examples of angular distribution results for few transitions in ^{84}Zr . Experimental data are shown by solid circles and results of the fit by solid lines.

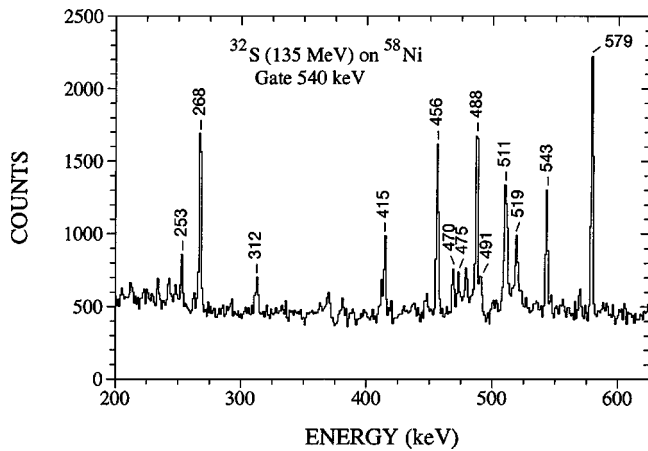


FIG. 4. Background-corrected spectrum of low-energy γ rays in prompt coincidence with the $2^+ \rightarrow 0^+$ 540 keV transition in ^{84}Zr , as extracted from the ^{32}S on ^{58}Ni in-beam measurement.

a higher-lying 4^- level by a 922.9 keV line supports the $\Delta I=2$ character, and thus, a spin of 4 is assigned to this level. No reliable DCO ratio could be extracted for the 852 keV line. However, the weak 603 keV line depopulating this level to the yrast 6^+ state supports a spin of possibly 6 for the 2740 keV level.

In summary, we have found evidence that all spins previously assigned to the $\Delta I=2$ sideband feeding into the 1575.3 keV level have to be reduced by one unit due to the following reasons: (i) The DCO ratios of the 456.2 and 1035.8 keV transitions can be interpreted as $\Delta I=1$ mixed dipole-quadrupole transitions. Considering the cross-linked levels and all measured DCO ratios, a firm assignment of spin 3 can be made to the 1575.3 keV level and, accordingly, odd spins to the known level sequence. (ii) The previous assignment of 14^+ to the state at 6248.2 keV makes this state yrast compared to the 14^+ state at 6302.1 keV of the well-established ground-state band. However, this is not compatible with the weak population of the 6248.2 keV state observed in both experiments. Our new assignment of 13^+ to the 6248.2 keV level resolves this problem. (iii) An alternative sequence involving the 768.5 and 852 keV transitions

has been identified and assigned as the even-spin level sequence of the γ -vibrational band.

2. Low-lying negative-parity states

A 267.7 keV γ transition has been found in strong coincidence with the known 1235.8 keV line, establishing a new level at 3078.8 keV. This level also decays by a 253.1 keV line to the known 5^- state at 2825.8 keV. Both low-energy transitions can be seen in the 540 keV gated coincidence spectrum displayed in Fig. 4. Previously, a 271 keV line was reported [5] which was placed in a similar way to the present 267.7 keV line; however, the given energies did not match up. The new level at 3078.8 keV is cross-linked to several other known states in ^{84}Zr , increasing our confidence in the indicated placement. DCO ratios for the 253.1 and 267.7 keV transitions (see Table I) indicate $\Delta I=1$ and 2 character, respectively, leading to spin assignments of 6 and 4 to the levels at 3078.8 and 2810.8 keV, respectively. Negative parity has been assigned to the 3078.8 keV level due to the 957.9 keV linking transition from the 8^- 4036.7 keV level. Negative parity then follows for the 2810.8 keV state because of the $E2$ multipolarity of the 267.7 keV transition. An $E2$ transition of this low energy might indicate a ns lifetime of the 3078.8 keV level, which could not be deduced from the data due to low statistics in the LEPS time spectra.

For the first time, a 1415.5 keV γ line has been found to feed into the yrast sequence of ^{84}Zr at spin 6. The coincidence relationships with the lower-lying yrast transitions are unambiguous. Thus, a new level at 3551.7 keV has been found. The DCO ratio of the 1415.5 keV line proves a $\Delta I=1$ transition, leading to a spin-7 assignment. It should be noted that the 1415.5 keV line is a close-lying doublet in the total coincidence matrix. Transitions at energies of 1415 and 1416 keV are known to be present in the neighboring odd-mass nucleus ^{83}Y [7,22]. The present placement in the level scheme has been made after a careful identification of all observed coincidence relationships.

The new 3551.7 keV state is depopulated also by a weak 726.4 keV transition to the known 5^- state at 2825.8 keV and is fed by a 826.9 keV transition connecting the level to the known 9^- state. Since $M2$ transitions are extremely un-

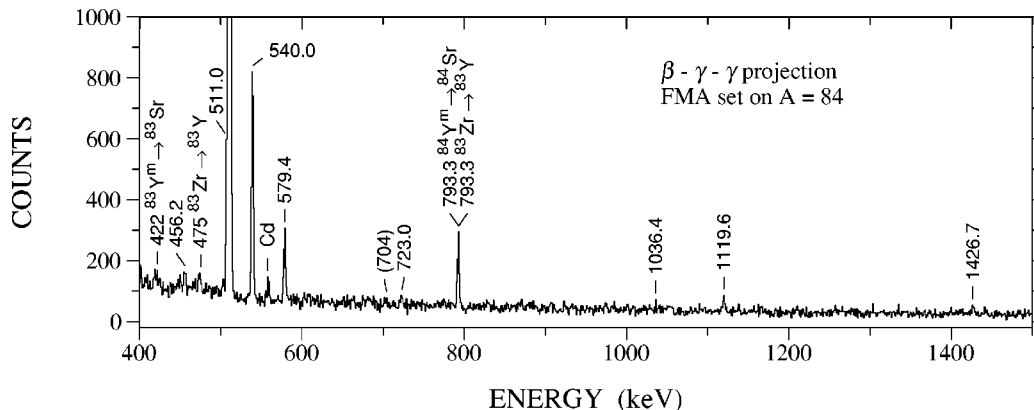


FIG. 5. Projection of the β -gated γ - γ matrix. The $A=84$ recoils were mass separated and transported to the counter station via a tape system. The label Cd represents the 558.46 keV transition in ^{114}Cd arising from the $^{113}\text{Cd}(n, \gamma)$ neutron capture reaction [18] in a thin sheet of natural Cd which was placed around the Ge detectors to suppress Pb x rays.

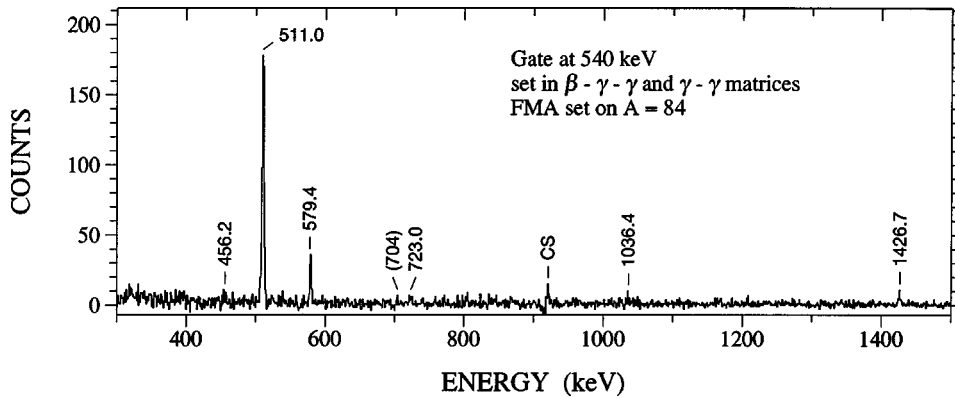


FIG. 6. Background-corrected spectrum of γ rays in coincidence with the 540 keV transition in ^{84}Zr as observed in the β decay of ^{84}Nb . The spectrum has been generated from the total γ - γ matrix (β - γ - γ plus γ - γ matrices). The letters CS label Compton scattering of the 1460.8 keV background line arising from the $^{40}\text{K} \rightarrow ^{40}\text{Ar}$ decay.

likely, these two $\Delta I=2$ transitions connecting the new state with known negative-parity states provide a negative-parity assignment for the 3551.7 keV level. The 3551.7 keV 7^- level may represent the head for a new band structure, resembling similar structures in other $N=44$ isotones such as ^{80}Kr [23] and ^{82}Sr [21] where three 7^- states were found. However, it is difficult to identify additional transitions feeding into the 3551.7 keV level due to the complexity of the 1415 keV peak in the total coincidence matrix.

A third 7^- state might be the new level at 3722 keV which depopulates via a 1586 keV transition to the 6^+ yrast level. Spin and parity assignments are tentatively given based on the weak 656 keV linking transition to the 9^- level at 4378.5 keV.

$(1, 2, 3)^+ \quad 0.0 \quad T_{1/2} = 9.5 \text{ s}$

$^{84}\text{Nb}_{41}$

$\beta^+/\text{EC} \quad Q = 9610 \text{ keV}$

BR (%) $\log f_0 t$

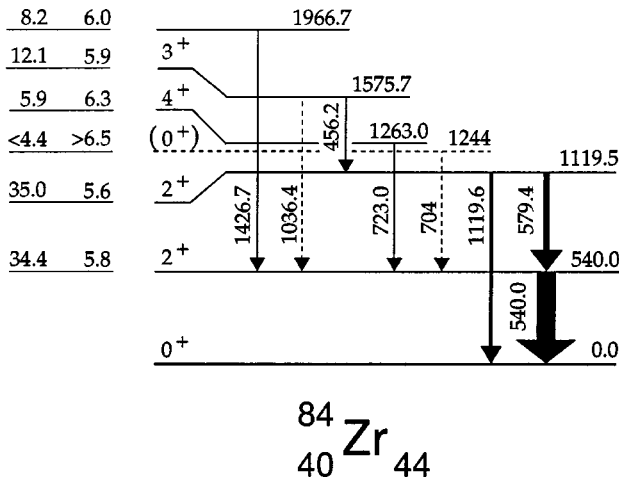


FIG. 7. Decay scheme of $^{84}\text{Nb} \rightarrow ^{84}\text{Zr}$ as deduced from the present study. Spin and parity assignments given for ^{84}Zr levels are based on the present decay and in-beam work. The transitions shown by a dashed line have been placed tentatively.

B. Level scheme of ^{84}Zr deduced from the ^{84}Nb decay

In our β -decay measurement only very few β - γ and γ - γ coincidences were observed. A representative γ -ray spectrum is shown in Fig. 5. The strongest lines in the spectrum are the 511.0 keV annihilation peak and the 540.0 keV $2^+ \rightarrow 0^+$ transition in ^{84}Zr [1,13]. Figure 6 shows the coincidence spectrum resulting from a gate set on the 540 keV line. There is clear evidence for a coincidence with a 579.4 keV transition which is known from the present and previous in-beam experiments [1,4] to depopulate the second 2^+ state at 1119.5 keV. The population of this second 2^+ level has been seen in β decay for the first time. The previously reported 23% decay branch [13] to the 4^+ yrast state at 1263.0 keV which decays to the 2^+ yrast state by a 723.0 keV transition has been observed with only about 7% relative intensity.

The level scheme of ^{84}Zr deduced from the present decay data is shown in Fig. 7. Besides the observation of the yrast 2^+ and 4^+ states, the level at 1575.7 keV has been seen in β^+/EC decay for the first time. It should be noted that the energy of the weak 1036.4 keV transition deviates by 0.7 keV from the energy difference, and thus, a tentative placement is given only. The assignment of the 456.2 keV transition to the ^{84}Nb decay is firm and a contamination through the 454.2 keV line [14] from the decay of the $^{83}\text{Y} \rightarrow ^{83}\text{Sr}$ channel can clearly be ruled out.

A new level at 1244 keV has been tentatively introduced based on a weak 540–704 keV coincidence measured in decay. The 704 keV γ ray has not been seen in previous decay nor in-beam experiments. It is likely that this line depopulates the second 0^+ state in ^{84}Zr . The proposed spin and parity assignments are, however, entirely based on systematics.

The half-life of the ^{84}Nb ground-state decay has been remeasured by analyzing the background-corrected β - γ time distribution of the 540.0 keV line which is shown in Fig. 8. A half-life of $9.5 \pm 1.0 \text{ s}$ has been obtained from a fit of a single-exponential decay curve to the experimental points. Our value is in fair agreement with the previously reported half-life of $12 \pm 3 \text{ s}$ [13].

Determination of logft values

For the calculation of the $\log ft$ values a Q_{EC} value of 9610 keV has been used. This value has been extracted from the mass excesses given in Ref. [15]. It should be noted that

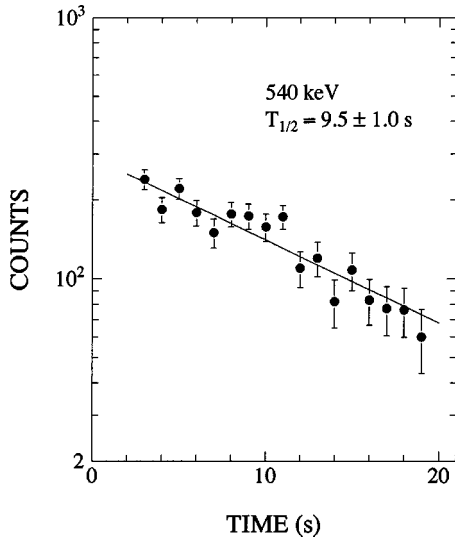


FIG. 8. Background-corrected decay curve of the 540 keV transition in ^{84}Zr . The time information obtained from the β - γ , β - γ - γ , and γ - γ events has been added up.

a recent experiment determined the ^{84}Nb mass by an end-point measurement of γ -gated β spectra to $Q_{\text{EC}} = 7200(300)$ keV [24]. This value is inconsistent with mass models and systematic trends [15]. The β - γ coincidence technique is known to sometimes produce incorrect mass measurements when the decay has a large Q_{EC} value, because the β decay is likely to proceed through many highly excited daughter states, giving rise to many lower energy β 's. This situation was found for the decay of the odd-odd nucleus ^{80}Y [25], where a discrepancy was encountered in Q_{EC} values determined by means of the end-point method [24] and a direct mass measurement [26].

The $\log ft$ values have been calculated based on branching ratios deduced from the relative intensities given in Table III and the new half-life of 9.5 s. They are given in Fig. 7 and Table IV. It is difficult to estimate the β branch directly populating the ^{84}Zr ground state. In general, the relatively weak occurrence of all ^{84}Zr lines compared to a similar measurement of the $N=Z+2$ ^{80}Y nucleus [25] may indicate some direct ground-state feeding. However, the calculation of the $\log ft$ values has been carried out with the assumption of no direct ground-state feeding. Also, energetically allowed, but so far unobserved, β decays to higher-lying levels in ^{84}Zr could reduce the observed β feeding to the known levels.

IV. DISCUSSION

Previously, a high degree of collectivity was found for the positive-parity yrast sequence in ^{84}Zr based on lifetime measurements. Over the years, lifetime values for the 2^+ state at 540 keV of $\tau = 24(2)$ ps [3], 20.3(11) ps [1], 17.8(11) ps [27], and 14.4(7) ps [11] were measured which lead to reduced $E2$ transition probabilities between 33(3) and 56(3) W.u. for the $2^+ \rightarrow 0^+$ transition supporting the deformed shape. In the following, the properties of the low- to medium-spin states are discussed in terms of the interplay

TABLE III. Energy levels and γ transitions assigned to the ^{84}Zr nucleus as observed in the radioactive decay of ^{84}Nb .

$E_{\text{lev}}^{\text{a}}$ (keV)	$I_i^{\pi \text{b}}$	$I_f^{\pi \text{b}}$	E_{γ}^{c} (keV)	I_{γ}
540.0	2^+	0^+	540.0(1)	100(2) ^d
1119.5	2_2^+	2^+	579.4(1)	34(2)
		0^+	1119.6(2)	13(2)
1244	(0_2^+)	2^+	704(1)	<5
1263.0	4^+	2^+	723.0(3)	6.7(17)
1575.7	3^+	2_2^+	456.2(2)	7.6(12)
		2^+	1036.4(5)	6.1(15)
1966.7		2^+	1426.7(3)	9.3(15)

^aEnergy of the initial state.

^bSpin and parity of initial and final states.

^cEnergy uncertainty is given in parentheses in units of the last digit.

^dNormalization.

between rotational and vibrational collectivities.

A. γ -vibrational band and triaxiality

The low-lying levels in some neutron-deficient even-even Zr isotopes deduced from β -decay studies and in-beam work are compiled in Fig. 9. The lowering of the yrast 2^+ , 4^+ , and 6^+ level energies with decreasing neutron number reflects the transition from an almost spherical shape in $^{86,88}\text{Zr}$ to a well-deformed shape with about $\beta_2 \approx 0.4$ in ^{80}Zr [28,29].

Several nonyrast positive-parity levels in ^{84}Zr have been grouped into a γ -vibrational band which is built on the second 2^+ state at 1119.2 keV. The band assignment is based on the observed decay pattern and on systematics. A compilation of the known γ -vibrational states in $^{82,84,86}\text{Zr}$ and their decay modes is also displayed in Fig. 9.

In general, the excitation energies of the γ -vibrational band members are considered to reflect to some extent the evolution of the nuclear shape in a chain of nuclei when going from a spherical to a deformed shape. Such an evolution often means a transition from vibrational to rotational excitations through a region of considerable γ softness [34].

TABLE IV. Levels in ^{84}Zr populated in the β^+/EC decay of ^{84}Nb .

E_{lev} (keV)	I^{π}	Branching ^a (%)	$\log ft^{\text{a}}$	Branching ^b (%)	$\log ft^{\text{b}}$
0.0	0^+	0 ^c			
540.0	2^+	34.4	5.8	77	5.6
1119.5	2_2^+	35.0	5.6		
1244	(0_2^+)	<4.4	>6.5		
1263.0	4^+	5.9	6.3	23	5.9
1575.7	3^+	12.1	5.9		
1966.7		8.2	6.0		

^aPresent results. Program LOGFT provided by the Brookhaven Nuclear Data Center has been used. $\log ft$ values have been calculated with $Q_{\text{EC}} = 9610$ keV [15] and the measured $T_{1/2} = 9.5$ s.

^bReference [14].

^cNo ground-state feeding has been assumed.

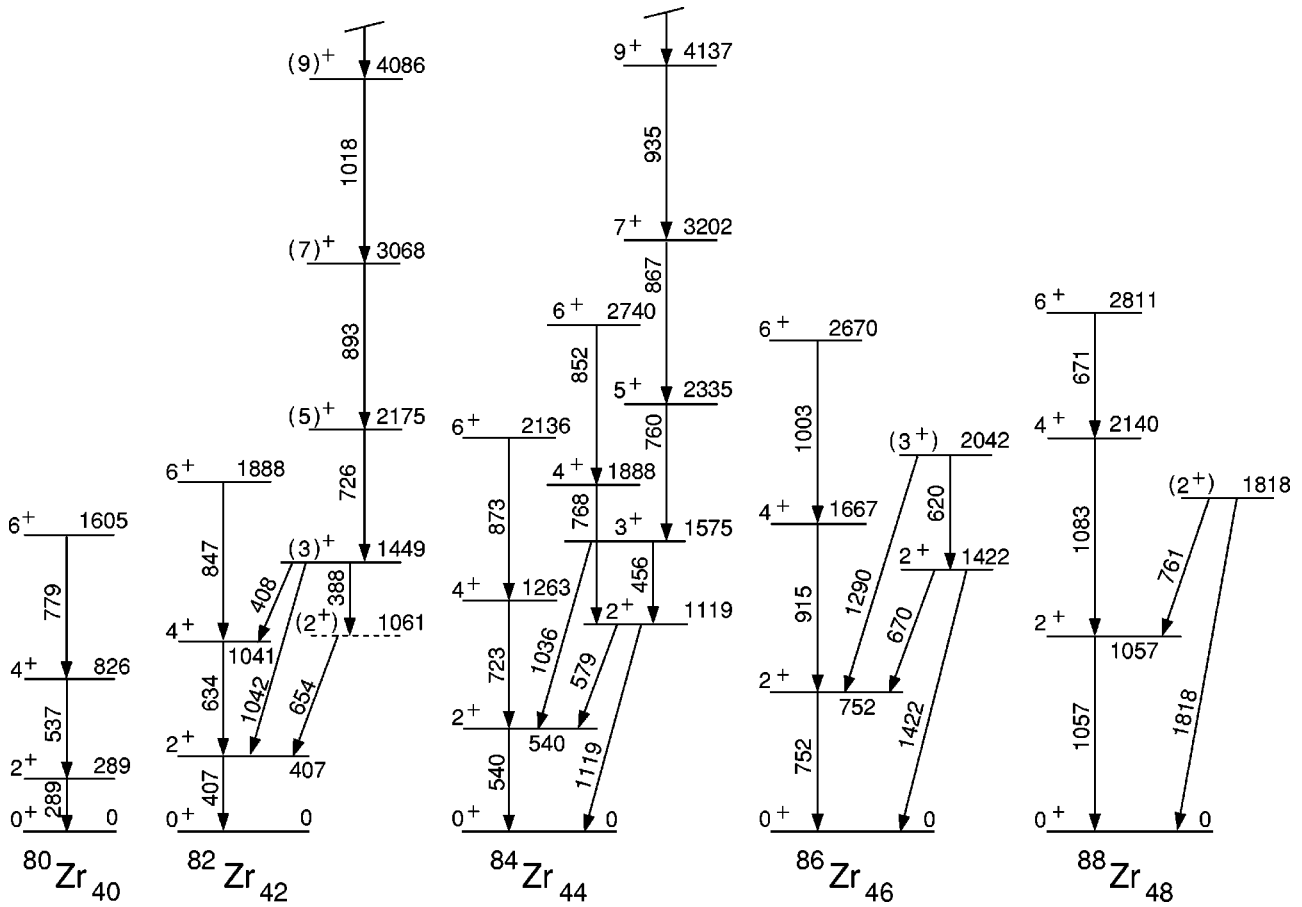


FIG. 9. Positive-parity yrast states with $I \leq 6$ in $^{80-88}\text{Zr}$ and states of the γ -vibrational bands built on the second 2^+ levels. The data have been taken from ^{80}Zr [28,29], ^{82}Zr [30], ^{86}Zr [31,32], and ^{88}Zr [33]. Note that not all γ decays are shown. In the ^{82}Zr level scheme [30], no spin assignment is given for the 1061 keV level; however, the present systematics points to a possible second 2^+ state at this energy. Thus, it is assumed in the present work.

Based on simple model considerations, transition energy ratios can be calculated for the states in the γ -vibrational bands. In a pure vibrational model, the energy separation of adjacent states is constant, leading to a normalized energy difference of 1 and 2 for $\Delta I = 1$ and 2 transitions, respectively [35]. In the approximation of a pure rotational model [35], the energy ratio is a linear function of the initial spin. Both tendencies have been displayed in Fig. 10 by dashed lines. The values deduced from the experimental energies of the γ -vibrational bands in $^{82,84}\text{Zr}$ and ^{82}Sr are displayed by solid symbols. One can see that the experimental values for ^{84}Zr are closer to the vibrational limit. Thus, the data points indicate a shape coexistence picture for ^{84}Zr , a deformed prolate shape for the lowest positive-parity yrast states, and a weakly deformed (γ -soft) shape for the low-lying states of the γ -vibrational band.

In terms of a γ -fluctuating triaxial rotor model [36], the γ softness of the potential is represented by the energy of the second 2^+ bandhead energy. The softer the nucleus, the lower is the energy of the second 2^+ state relative to the yrast 4^+ state [36], and thus the smaller becomes the energy ratio $E(2_2^+)/E(4^+)$. Experimental values of 1.02, 0.89, and 0.85 can be deduced for the $^{82,84,86}\text{Zr}$ nuclei and 1.16, 0.88, and 0.82 for the $^{80,82,84}\text{Sr}$ nuclei. The observed pattern

clearly indicates the tendency of increasing γ softness with increasing neutron number for both chains. Thus, this tendency reflects the increasing influence of the spherical $N = 50$ neutron shell closure.

In the rotational model, the second 2^+ state forms the head of the collective γ -vibrational band, and a low-lying 3^+ state is predicted. This 3^+ level corresponds very likely to the level at 1575.3 keV in ^{84}Zr . Based on the $3^+ \rightarrow 2^+$ transition energy of 456.2 keV, the moment of inertia is smaller in the γ -vibrational band compared to the ground-state band, indicating a less deformed shape. It should be mentioned that the 3^+ assignment to the 1575.3 keV level in ^{84}Zr fits well into the systematics, as opposed to the previously reported 4^+ assignment.

A distinction between excitations in a γ -soft and a γ -rigid potential can be deduced from the γ -band level energy separation and can be expressed in the staggering function $S(4,3,2)$ [37]. Experimental values of $S(4,3,2)$ for some even-even Kr, Sr, and Zr nuclei are displayed in Fig. 11 as function of the neutron number. They all lie in the range from -0.7 to -0.1 . Theoretical values of the $S(4,3,2)$ function vary between 0.3 and -2.0 for a γ -soft rotor. Thus, the experimental values may imply a γ -soft rotor with a triaxiality of about 25° for ^{84}Zr , similar to the conclusion found

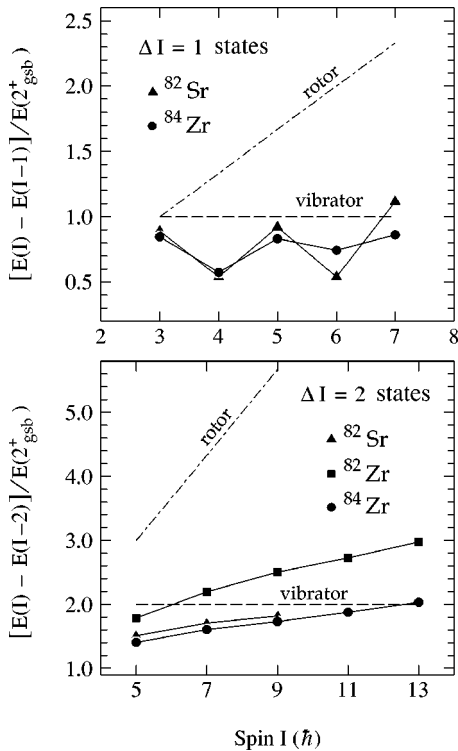


FIG. 10. Normalized energy difference for $\Delta I=1$ (top) and $\Delta I=2$ (bottom) states in the γ -vibrational bands of $^{82,84}\text{Zr}$ and ^{82}Sr as a function of the initial spin of the state. The predicted ratios for a pure vibrational and a pure rotational behavior are given by dashed and dash-dotted lines, respectively. For normalization the 2^+ energy of the ground-state band (gsb) of the respective Zr or Sr nuclei has been taken.

recently for ^{80}Sr [25]. Note that the triaxiality parameter γ is defined in Ref. [37] as $\gamma=0^\circ$ and $\gamma=+60^\circ$ for prolate and oblate shapes, respectively.

B. Evolution of the nuclear shape at low spins in ^{84}Zr

Total Routhian surface (TRS) calculations [38] have been performed to probe the evolution of the nuclear shape as a function of the rotational frequency. The calculations were carried out using a Woods-Saxon potential for the single-particle energies and a monopole-type pairing force. At each grid point the energy was minimized with regard to the hexadecapole deformation. Results from these calculations are shown in Fig. 12 for low-lying positive-parity states. The TRS plots are composed of various (collective) configurations specified in terms of parity and signature quantum numbers, which compete in energy and thus reflect shape coexistence.

In the ground state (left panel of Fig. 12), the even-even nucleus ^{84}Zr exhibits a spherical nuclear shape, in agreement with previous calculations [6]. A deformed minimum lies about 800 keV higher in energy and is pretty shallow. At a rotational frequency of only about 0.29 MeV, a triaxial shape with $\beta_2=0.29$ and a triaxiality parameter of $\gamma=-24^\circ$ becomes lowest in energy, however, this shape is very γ soft. Thus, collective rotation quickly becomes energetically fa-

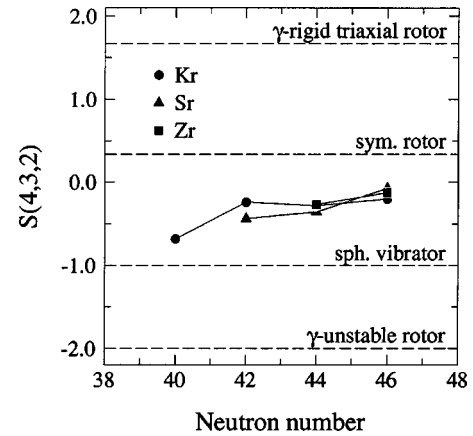


FIG. 11. Experimental values of the staggering function $S(4,3,2)$ deduced from known states in the γ -vibrational bands of even-even Kr, Sr, and Zr nuclei. Predictions of different models are shown by dashed horizontal lines. The sign convention of the triaxiality parameter γ is according to Ref. [37].

vorable, and the ground-state band of ^{84}Zr has been associated with this triaxial-deformed shape [6].

An additional minimum occurs in the middle panel of Fig. 12 at a lower quadrupole deformation of $\beta_2 \approx 0.15$ and $\gamma \approx 15^\circ$ which moves towards a near-prolate shape with increasing frequency. Even though in the proton-rich Zr nuclei experimental evidence for shape coexistence at low spins is less clear, it has been seen in the calculations that the 0^+ and partly the 2^+ states of the ground-state band are pushed down in energy, presumably due to an interaction with excited 0^+ and 2^+ states with smaller deformation. This low-spin shape coexistence is reflected in the middle and right panels of Fig. 12 by the occurrence of additional minima at reduced quadrupole deformation. Thus, one may identify the second minimum with the collective band built on the second 2^+ state. The calculated shape is very γ soft; however, the triaxiality of 25° deduced in the previous section (which corresponds to -25° in the TRS notation) is not reproduced.

C. Two-quasineutron excitations

The observation of the closely spaced 4^- and 6^- levels at 2810.8 and 3078.8 keV in ^{84}Zr , respectively, is somewhat surprising in light of the reported [1,3] large quadrupole deformation for this nucleus. A similar structure has also been seen in the moderately deformed nucleus ^{82}Sr [21] and in the less deformed nuclei ^{80}Kr [19,23] and ^{78}Se [20], all $N=44$ isotones to ^{84}Zr , as displayed in Fig. 13. In the lighter isotones ^{78}Se and ^{80}Kr , the measured $E2$ transition probabilities of 4(1) and 7(2) W.u. for the 271 and 249 keV $6^- \rightarrow 4^-$ transitions, respectively, verify a low collectivity. It is very likely, based on the similarity in the excitation energies and depopulation pattern, that this structure is preserved in ^{84}Zr , implying a low collectivity too. The relatively weak population of the 6^- state in our experiment, however, did not allow us to measure its lifetime.

The assumed low collectivity for the 4^- and 6^- states in ^{84}Zr and the nonobservation of a feeding high-spin band indicate a much reduced quadrupole deformation, where a possible triaxiality cannot be excluded. Since this negative-

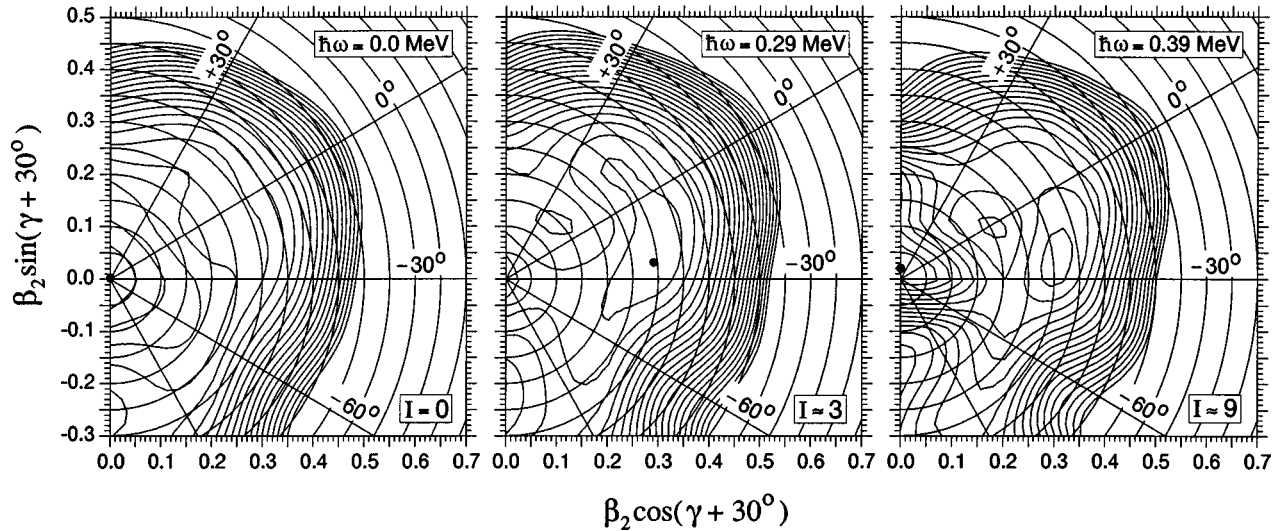


FIG. 12. Total Routhian surfaces calculated for positive-parity yrast states with signature $\alpha=0$ in ^{84}Zr and displayed in the (β_2, γ) polar coordinate plane. The rotational frequencies and the corresponding spins are given in the insets. The energy separation between contour lines is 200 keV. The absolute minimum is indicated by a solid dot. Collective prolate and collective oblate shapes correspond to triaxiality parameters of $\gamma=0^\circ$ and -60° , respectively.

parity structure persists at almost the same energy despite filling the proton $f_{5/2}$ and $p_{1/2}$ orbitals; i.e., across the sub-shell closure at $Z=38$, it is related to the 44 neutrons. For this neutron number and a relatively small (near-prolate) deformation, the Fermi level is close to the negative-parity $f_{5/2}$ and $p_{1/2}$ orbitals which are mixed by rotation. Thus, we interpret the observed 4^- and 6^- states as noncollective $(g_{9/2}, pf)$ two-quasineutron excitations, in contrast to the lowest states of the negative-parity bands 4 and 5 which have been identified as $(g_{9/2}, pf)$ two-quasiproton excitations at a near-prolate shape with $\beta_2 \approx 0.2$ [4]. Probably, the main components in the 4^- and 6^- states are two-quasiparticle configurations of the type $\nu(g_{9/2}, p_{1/2})$ and $\nu(g_{9/2}, f_{5/2})$, respectively, reflecting the small energy separation between the $1/2^-$ ground state and the lowest $5/2^-$ state in the odd-mass $N=43$ isotones ^{77}Se to ^{83}Zr .

In the isotope $^{86}\text{Mo}_{44}$, the depopulation of the $6^{(-)}$ state at 2959 keV occurs via a 242 keV transition to the $5^{(-)}$ state, and no 4^- state is known [39]. It seems that the nature of the negative-parity high-spin sequence changes its character between ^{84}Zr and ^{86}Mo . In the lighter isotones ^{82}Sr and ^{84}Zr , collective bands are built on the second 6^- states at 3339 and 3313.3 keV, respectively, which become negative-parity yrast sequences at the 8^- levels. These sequences have been observed up to high spins. Alignment properties and the extracted moments of inertia support the interpretation as collective states built on two-quasiproton excitations. In ^{86}Mo , a decay sequence has been found which is built on the lowest 6^- state with a different behavior of the moments of inertia when compared to ^{84}Zr ; see Fig. 4(c) in Ref. [39]. These moments of inertia indicate that the negative-parity sequence in ^{86}Mo is less collective than in ^{84}Zr . Thus, the decay sequence in ^{86}Mo reflects the influence of quasiparticle excitations which are present in the lowest 6^- state.

D. Spin and parity of the ^{84}Nb ground state

The strong apparent β feeding of the 2^+ and 2^+ levels at 540.0 and 1119.5 keV in ^{84}Zr , respectively, with $\log ft$ values below 6 indicates allowed transitions [40] and supports a positive-parity assignment for the ground state of ^{84}Nb . The spin is restricted to values of 1, 2, or 3. The $\log ft$ of the β branch to the 4^+ level at 1263.0 keV calculated with the assumption of no direct β feeding to the ground state appears to contradict possible spins of 1^+ or 2^+ and has led to the previous assignment of (3^+) [14]. However, the 723.0 keV line has been observed to be rather weak in the present decay work, and it is quite possible that the 4^+ state is fed primarily by γ decays from higher-lying levels populated by unobserved β branches. Also the new assignment of spin 3^+ to the more strongly populated 1575.7 keV level leaves both spins 2 and 3 possible for the ground state of ^{84}Nb .

On the other hand, a spin assignment of 1^+ to the ground state of ^{84}Nb would explain the low γ intensity associated with the β^+/EC decay of the $N=Z$ nucleus ^{84}Mo which should have been produced via the $^{58}\text{Ni}(^{28}\text{Si}, 2n)$ reaction [41,42]. The production cross section for ^{84}Mo was estimated to be $7(3) \mu\text{b}$ [41]. If we assume a 1^+ assignment, then the 0^+ ground state of ^{84}Mo can easily be depopulated by an allowed β branch to the ground state of ^{84}Nb . Further, the β decay of ^{84}Nb can proceed through an allowed transition to the ground state of ^{84}Zr , similar to the 75(25)% branch observed in the β decay of the 1^+ ground-state decay of the isotope ^{82}Y [43]. In conclusion, the spin of the ground state of ^{84}Nb remains an open question, and spin-parity values of 1^+ , 2^+ , or 3^+ are all possible, depending on which, if any, β -decay branches have not been observed.

V. SUMMARY AND CONCLUSIONS

The low- to medium-spin structure of the even-even nucleus ^{84}Zr has been reinvestigated via the $^{58}\text{Ni}(^{32}\text{S}, \alpha 2p)$

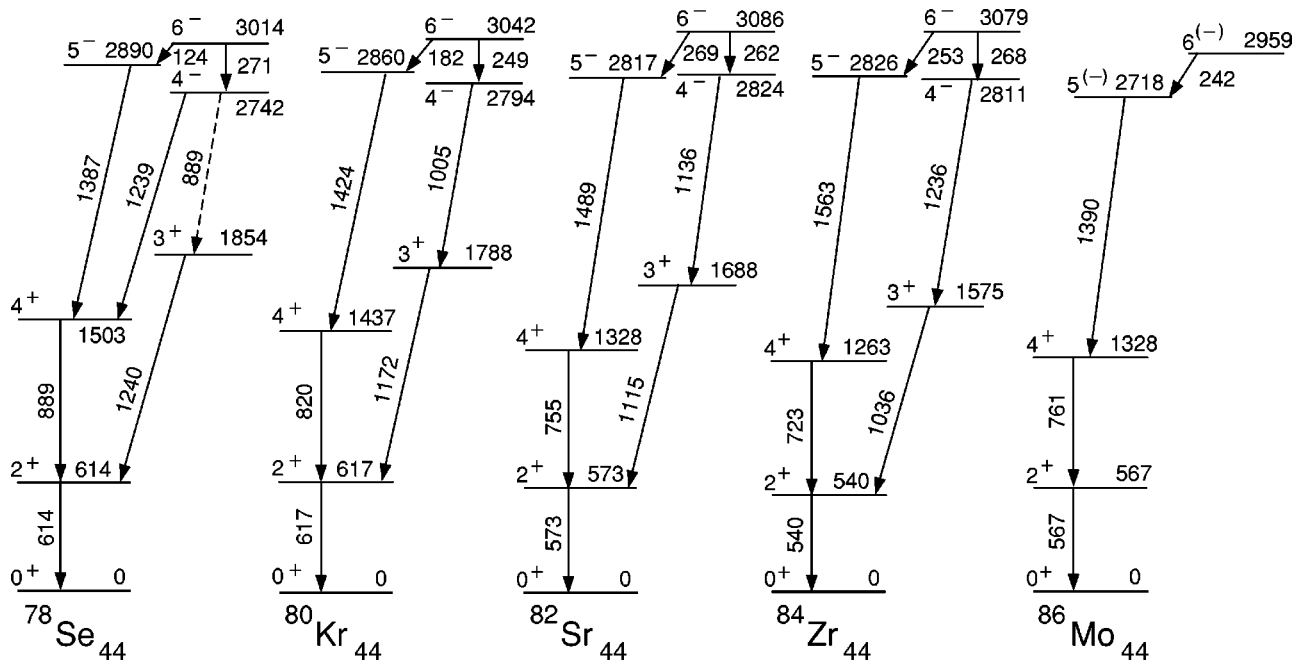


FIG. 13. Systematics of experimental energies of the lowest 4^- , 5^- , and 6^- states and some of their γ decays to lower-lying states in selected $N=44$ isotones. The experimental data were taken from ^{78}Se [20], ^{80}Kr [19,23], ^{82}Sr [21], and ^{86}Mo [39].

and $^{59}\text{Co}(^{28}\text{Si}, p2n)$ reactions by using a five-Ge-detector plus LEPS setup at the Nuclear Structure Laboratory at Florida State University. Several new levels related to the γ -vibrational band have been found, in particular the even-spin sequence. Further, new spin assignments have been made for the previously reported members of this band based on our DCO ratios and an angular distribution measurement. Thus, the γ -vibrational band in ^{84}Zr is now known in greatest detail when compared to other neutron-deficient Zr isotopes. This provides a unique opportunity to infer the degree of triaxiality.

As a result of our new assignment of 3^+ to the 1575.3 keV level, the previously known even-spin sequence has been converted into an odd-spin sequence. This fits well into the systematics, and the previously reported 14^+ yrast state in this band becomes a 13^+ assignment. Systematics of energy separations in the γ -vibrational bands of $^{82,84}\text{Zr}$ indicate an increasing γ softness with increasing neutron number as verified from the energy of the second 2^+ bandhead state and the staggering function $S(4,3,2)$. This behavior of the proton-rich even-even Zr isotopes resembles that of the proton-rich even-even Sr isotopes.

The radioactive decay of mass-separated ^{84}Nb sources has also been studied. The sources were produced by bombarding a ^{58}Ni target with a beam of 94 MeV ^{28}Si ions,

separated from other reaction products through the Argonne fragment mass analyzer and measured with a β - γ detector setup. Several low-lying states in ^{84}Zr have been identified, and a half-life of 9.5 ± 1.0 s has been measured for the ^{84}Nb ground-state β decay. The extracted $\log ft$ values and possible uncertainties due to unobserved branches restrict the spin and parity of the ^{84}Nb ground state to 1^+ , 2^+ , or 3^+ . Additional decay experiments are necessary to determine the spin value of the ^{84}Nb ground state with higher confidence.

ACKNOWLEDGMENTS

The authors appreciate the on-line service of the National Nuclear Data Center, Brookhaven National Laboratory, for providing the code for the $\log ft$ calculations. We are grateful to W. Nazarewicz and R. Wyss for providing the computer codes and data files for the TRS calculations, and to H. Grawe for illuminating discussions regarding the nuclear shell model. The nuclear physics research was supported by the National Science Foundation at Florida State University under Grant No. PHY 95-23974 and at the University of Notre Dame under Grant No. PHY 94-02761, and by the Division of High Energy and Nuclear Physics of the U.S. Department of Energy at Argonne National Laboratory under Contract No. W-31-109-ENG-38 and at the University of Maryland under Grant No. DE-FG02-94-ER40834.

- [1] H.G. Price, C.J. Lister, B.J. Varley, W. Gelletly, and J.W. O'neess, Phys. Rev. Lett. **51**, 1842 (1983).
 [2] A.W. Mountford, J. Billowes, W. Gelletly, H.G. Price, and D.D. Warner, Phys. Lett. B **279**, 228 (1992).
 [3] S. Chattopadhyay, H.C. Jain, and J.A. Sheikh, Phys. Rev. C **53**,

- 1001 (1996).
 [4] A.A. Chishti, P. Chowdhury, D.J. Blumenthal, P.J. Ennis, C.J. Lister, C. Winter, D. Vretenar, G. Bonsignori, and M. Savoia, Phys. Rev. C **48**, 2607 (1993).
 [5] H.-Q. Jin, C. Baktash, M.J. Brinkman, C.J. Gross, D.G. Saran-

- tites, I.Y. Lee, B. Cederwall, F. Cristancho, J. Döring, F.E. Durham, P.-F. Hua, G.D. Johns, M. Korolija, D.R. LaFosse, E. Landolfo, A.O. Macchiavelli, W. Rathbun, J.X. Saladin, D.W. Stracener, S.L. Tabor, and T.R. Werner, *Phys. Rev. Lett.* **75**, 1471 (1995).
- [6] J. Dudek, W. Nazarewicz, and N. Rowley, *Phys. Rev. C* **35**, 1489 (1987).
- [7] T.D. Johnson, A. Aprahamian, C.J. Lister, D.J. Blumenthal, B. Crowell, P. Chowdhury, P. Fallon, and A.O. Macchiavelli, *Phys. Rev. C* **55**, 1108 (1997).
- [8] C. Teich, A. Jungclaus, V. Fischer, D. Kast, K.P. Lieb, C. Lingk, C. Ender, T. Härtlein, F. Köck, D. Schwalm, J. Billowes, J. Eberth, and H.G. Thomas, *Phys. Rev. C* **59**, 1943 (1999).
- [9] R.A. Kaye, J.B. Adams, A. Hale, C. Smith, G.Z. Solomon, S.L. Tabor, G. Garcia-Bermúdez, M.A. Cardona, A. Filevich, and L. Szybisz, *Phys. Rev. C* **57**, 2189 (1998).
- [10] P. Chowdhury, C.J. Lister, D. Vretenar, C. Winter, V.P. Janzen, H.R. Andrews, D.J. Blumenthal, B. Crowell, T. Drake, P.J. Ennis, A. Galindo-Uribarri, D. Horn, J.K. Johansson, A. Omar, S. Pilotte, D. Prévost, D. Radford, J.C. Waddington, and D. Ward, *Phys. Rev. Lett.* **67**, 2950 (1991).
- [11] A. Jungclaus, K.P. Lieb, C.J. Gross, J. Heese, D. Rudolph, D.J. Blumenthal, P. Chowdhury, P.J. Ennis, C.J. Lister, C. Winter, J. Eberth, S. Skoda, M.A. Bentley, W. Gelletly, and B.J. Varley, *Z. Phys. A* **340**, 125 (1991).
- [12] C.N. Davids, B.B. Back, K. Bindra, D.J. Henderson, W. Kutschera, T. Lauritsen, Y. Nagame, P. Sugathan, A.V. Ramayya, and W.B. Walters, *Nucl. Instrum. Methods Phys. Res. B* **70**, 358 (1992).
- [13] G. Korschinek, E. Nolte, H. Hick, K. Miyano, W. Kutschera, and H. Morinaga, *Z. Phys. A* **281**, 409 (1977).
- [14] R. B. Firestone and V. S. Shirley, *Table of Isotopes*, 8th ed. (Wiley, New York, 1996).
- [15] G. Audi, O. Bersillon, J. Blachot, and A.H. Wapstra, *Nucl. Phys.* **A624**, 1 (1997).
- [16] S.L. Tabor, *Nucl. Instrum. Methods Phys. Res. A* **265**, 495 (1988).
- [17] K.S. Krane, R.M. Steffen, and R.M. Wheeler, *Nucl. Data Tables* **11**, 351 (1973).
- [18] J. Blachot and G. Marguier, *Nucl. Data Sheets* **60**, 139 (1990).
- [19] L. Funke, J. Döring, F. Dubbers, P. Kemnitz, E. Will, G. Winter, V.G. Kiptilij, M.F. Kudojarov, I.K. Lemberg, A.A. Pasternak, A.S. Mishin, L. Hildingsson, A. Johnson, and T. Lindblad, *Nucl. Phys.* **A355**, 228 (1981).
- [20] R. Schwengner, G. Winter, J. Döring, L. Funke, P. Kemnitz, E. Will, A.E. Sobov, A.D. Efimov, M.F. Kudojarov, I.K. Lemberg, A.S. Mishin, A.A. Pasternak, L.A. Rassadin, and I.N. Chugunov, *Z. Phys. A* **326**, 287 (1987).
- [21] S.L. Tabor, J. Döring, J.W. Holcomb, G.D. Johns, T.D. Johnson, T.J. Petters, M.A. Riley, and P.C. Womble, *Phys. Rev. C* **49**, 730 (1994).
- [22] F. Cristancho, C.J. Gross, K.P. Lieb, D. Rudolph, Ö. Skeppstedt, M.A. Bentley, W. Gelletly, H.G. Price, J. Simpson, J.L. Durell, B.J. Varley, and S. Rastikerdar, *Nucl. Phys.* **A540**, 307 (1992).
- [23] J. Döring, V.A. Wood, J.W. Holcomb, G.D. Johns, T.D. Johnson, M.A. Riley, G.N. Sylvan, P.C. Womble, and S.L. Tabor, *Phys. Rev. C* **52**, 76 (1995).
- [24] M. Shibata, A. Odahara, S. Mitarai, Y. Gono, M. Kidera, K. Miyazaki, and T. Kuroyanagi, *J. Phys. Soc. Jpn.* **65**, 3172 (1996).
- [25] J. Döring, A. Aprahamian, R.C. de Haan, J. Görres, H. Schatz, M. Wiescher, W.B. Walters, L.T. Brown, C.N. Davids, C.J. Lister, and D. Seweryniak, *Phys. Rev. C* **59**, 59 (1999).
- [26] S. Issmer, M. Fruneau, J.A. Pinston, M. Asghar, D. Barnéoud, J. Genevey, T. Kerscher, and K.E.G. Löbner, *Eur. Phys. J. A* **2**, 173 (1998).
- [27] C.J. Lister, B.J. Varley, W. Fieber, J. Heese, K.P. Lieb, E.K. Warburton, and J.W. Olness, *Z. Phys. A* **329**, 413 (1988).
- [28] C.J. Lister, M. Campbell, A.A. Chishti, W. Gelletly, L. Goettig, R. Moscrop, B.J. Varley, A.N. James, T. Morrison, H.G. Price, J. Simpson, K. Connel, and O. Skeppstedt, *Phys. Rev. Lett.* **59**, 1270 (1987).
- [29] C. J. Lister, S. M. Fisher, and D. P. Balamuth, in *Proceedings of the International Workshop on Selected Topics on $N=Z$ Nuclei*, edited by D. Rudolph and M. Hellström, Report No. LUIP0003, Bloms i Lund, 2000, p. 46.
- [30] D. Rudolph, C. Baktash, C.J. Gross, W. Satula, R. Wyss, I. Birriel, M. Devlin, H.-Q. Jin, D.R. LaFosse, F. Lerma, J.X. Saladin, D.G. Sarantites, G.N. Sylvan, S.L. Tabor, D.F. Winchell, V.Q. Wood, and C.H. Yu, *Phys. Rev. C* **56**, 98 (1997).
- [31] J. Hattula, S. Juutinen, H. Helppi, A. Pakkanen, M. Piiparinen, S. Elfström, and T. Lindblad, *Phys. Rev. C* **28**, 1860 (1983).
- [32] E.K. Warburton, C.J. Lister, J.W. Olness, P.E. Haustein, S.K. Saha, D.E. Alburger, J.A. Becker, R.A. Dewberry, and R.A. Naumann, *Phys. Rev. C* **31**, 1211 (1985).
- [33] H.-W. Müller, *Nucl. Data Sheets* **54**, 1 (1988).
- [34] M. Sakai, *Nucl. Phys.* **A104**, 301 (1967).
- [35] N. Yoshikawa, Y. Shida, O. Hashimoto, M. Sakai, and T. Numao, *Nucl. Phys.* **A327**, 477 (1979).
- [36] N. Onishi, I. Hamamoto, S. Åberg, and A. Ikeda, *Nucl. Phys.* **A452**, 71 (1986).
- [37] N.V. Zamfir and R.F. Casten, *Phys. Lett. B* **260**, 265 (1991).
- [38] W. Nazarewicz, J. Dudek, R. Bengtsson, T. Bengtsson, and I. Ragnarsson, *Nucl. Phys.* **A435**, 397 (1985).
- [39] D. Rudolph, C.J. Gross, Y.A. Akaoli, C. Baktash, J. Döring, F.E. Durham, P.-F. Hua, G.D. Johns, M. Korolija, D.R. LaFosse, I.Y. Lee, A.O. Macchiavelli, W. Rathbun, D.G. Sarantites, D.W. Stracener, S.L. Tabor, A.V. Afanasjev, and I. Ragnarsson, *Phys. Rev. C* **54**, 117 (1996).
- [40] S. Raman and N.B. Gove, *Phys. Rev. C* **7**, 1995 (1973).
- [41] W. Gelletly, M.A. Bentley, H.G. Price, J. Simpson, C.J. Gross, J.L. Durell, B.J. Varley, O. Skeppstedt, and S. Rastikerdar, *Phys. Lett. B* **253**, 287 (1991).
- [42] D. Bucurescu, C. Rossi Alvarez, C.A. Ur, N. Mărginean, P. Spolaore, D. Bazzacco, S. Lunardi, D.R. Napoli, M. Ionescu-Bujor, A. Iordăchescu, C.M. Petrache, G. de Angelis, A. Gadea, D. Foltescu, F. Brandolini, G. Falconi, E. Farnea, S.M. Lenzi, N.H. Medina, Z. Podolyak, M. De Poli, M.N. Rao, and R. Venturelli, *Phys. Rev. C* **56**, 2497 (1997).
- [43] M. Oinonen, R. Béraud, G. Cachel, E. Chabanat, P. Den- dooven, A. Emsallem, S. Hankonen, A. Honkanen, J. Huikari, A. Jokinen, G. Lhersonneau, C. Miehé, A. Nieminen, Y. Novikov, H. Penttilä, K. Peräjärvi, A. Popov, D.M. Seliverstov, J.C. Wang, and J. Aystö, *Nucl. Instrum. Methods Phys. Res. A* **416**, 485 (1998).